

# Experimental study of single-electron loss by $\text{Ar}^+$ ions in rare-gas atoms

P G Reyes<sup>1</sup>, F Castillo<sup>2</sup> and H Martínez<sup>3</sup>

<sup>1</sup> Facultad de Ciencias, UNAM, Coyoacan, México and Estudiante de Doctorado de la Facultad de Ciencias, UAEMex, Mexico

<sup>2</sup> Instituto de Ciencias Nucleares, UNAM, Coyoacan, Mexico

<sup>3</sup> Centro de Ciencias Físicas, UNAM, Apdo Postal 48-3, 62251 Cuernavaca, Morelos, Mexico

E-mail: hm@fis.unam.mx

Received 9 October 2000, in final form 13 February 2001

## Abstract

Absolute differential and total cross sections for single-electron loss were measured for  $\text{Ar}^+$  ions on rare-gas atoms in the laboratory energy range of 1.5 to 5.0 keV. The electron loss cross sections for all the targets studied are found to be in the order of magnitude between  $10^{-19}$  and  $10^{-22}$  cm<sup>2</sup>, and show a monotonically increasing behaviour as a function of the incident energy. The behaviour of the total single-electron loss cross sections with the atomic target number,  $Z_t$ , shows different dependences as the collision energy increases. In all cases the present results display experimental evidence of saturation in the single-electron loss cross section as the atomic number of the target increases.

## 1. Introduction

In ion–atom collisions to date, most of the experimental and theoretical studies of electron loss have involved the simplest case of light projectiles colliding with various atoms and molecules (Jalowy *et al* 2000, Ogawa *et al* 2000, Melo *et al* 1999, Kolakowska and Pindzola 1999, Saha *et al* 1999, Voitkiv *et al* 1999, Sant’Anna *et al* 1998, Montenegro *et al* 1994, Kaneko 1985, 1986, Wu *et al* 1997) and even these are often restricted to the high-velocity regime. In the low and moderate energy range, there are few previous measurements of single-electron loss of  $\text{Ar}^+$  with rare gases (Martínez 1998, Jones *et al* 1959, Dmitriev *et al* 1962, Kaminker and Fedorenko 1955, Müller *et al* 1976, Fedorenko *et al* 1957, Bliman *et al* 1980), while to understand the electron dynamics in low-energy collisions a detailed molecular description is required, in which the crossings between molecular states and the coupling of these states with the continuum play a fundamental role (Delos 1981, Barat and Lichten 1972, Lichten 1967, Brenot *et al* 1975, Sidis *et al* 1975). In the analysis of the measured data of inelastic processes in symmetric atom–atom collisions for rare-gas atoms, Brenot (1975) concluded that in a first approximation, these processes seem to occur through the same basic mechanism in the atom–atom and ion–atom cases. In the Kr–Kr case they reported for 3 keV, the differential ionization cross sections for the projectile and ionization of the projectile

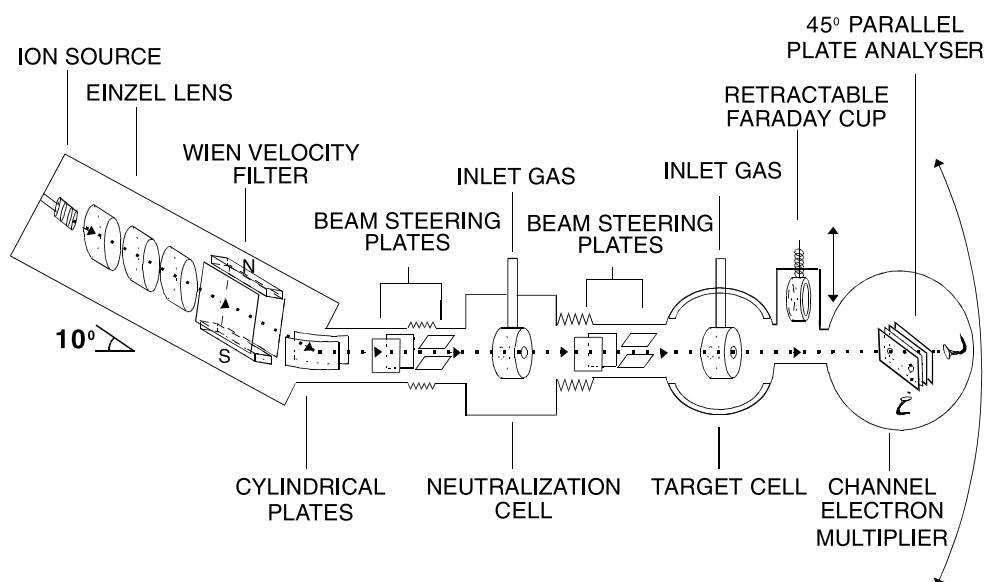


Figure 1. Schematic diagram of the apparatus.

with excitation of the target. They considered that the promotion of one electron from the  $6h\sigma_u$  molecular orbital (MO) was the main mechanism. Also, an understanding of loss processes at low collision energies has become increasingly important in a number of applications such as plasma physics (Janev 1995), atomic physics (Datz *et al* 1999), material science (Möller 1999) and radiotherapy and radiation research (Möller 1999). In previous works (Martínez 1998, 1999, Martínez *et al* 2000), the energy dependence of the single-electron loss cross section of  $\text{Ar}^+$ –He and  $\text{Kr}^+$ –He, –Ne, –Ar, –Kr, –Xe systems has been measured. Thus, to extend the single-electron loss studies to heavy atoms, we have conducted experiments that have determined the single-electron loss cross sections of  $\text{Ar}^+$  in  $\text{Ar}^+$ –atom collisions. To the best of our knowledge, for the  $\text{Ar}^+$ –Ne, –Kr, –Xe systems, these are the first measurements in this energy range. This paper is intended to acquire knowledge of the dependence of the single-electron loss cross sections of  $\text{Ar}^+$  on the physical parameters  $E$  (incident laboratory energy); that is  $\text{Ar}^+ + (\text{Ne}, \text{Ar}, \text{Kr}, \text{Xe}) \rightarrow \text{Ar}^{2+} + \dots$ , and  $Z_t$  (target atomic number), in order to obtain a consistent set of results. Data were measured for laboratory energies between 1.5 and 5.0 keV and for  $10 \leq Z_t \leq 54$ .

## 2. Experiment

The experimental apparatus and technique needed to generate the fast ion beam were recently reported (Martínez 1999, Martínez and Reyes 1999) and are displayed in figure 1. Briefly, the  $\text{Ar}^+$  ions formed in an arc discharge source containing Ar gas (99.99% purity) at ion source pressures of 0.05–0.08 mTorr were accelerated to 1.0–5.0 keV and selected by a Wien velocity filter. The  $\text{Ar}^+$  ions were then allowed to pass through a series of collimators before entering the gas target cell, which was a cylinder of 2.5 cm in length and diameter, with a 1 mm entrance aperture, and a 2 mm wide, 6 mm long exit aperture. This geometry permitted the measurements of the  $\text{Ar}^{2+}$ , the directions of which make an angle of up to  $\pm 7^\circ$ . Path lengths and apertures were chosen such that the root-mean-square angular resolution of the system

was  $\approx 0.1^\circ$ . All apertures and slits had knife edges. The target cell was located at the centre of a rotatable, computer controlled vacuum chamber that moved the whole detector assembly which was located 47 cm away from the target cell. A precision stepping motor ensured a high repeatability in the positioning of the chamber over a large series of measurements. The detector assembly consisted of a Harrower-type parallel-plate analyser and two channel-electron multipliers (CEMs) attached to its exit ends. The Ar<sup>0</sup> atoms passed straight through the analyser. Separation of charged particles occurred inside the analyser, which was set to detect the Ar<sup>2+</sup> ions ( $I_f(\theta)$ ) particles per unit solid angle ( $7.85 \times 10^{-7}$  sr) per second detected at a laboratory angle  $\theta$  with respect to the incident beam direction (typically  $\sim 1.5 \times 10^8$  particles/sr s) with the lateral CEM. The CEM was calibrated *in situ* with a low-intensity Ar<sup>2+</sup> beam, which was measured as a current in a Faraday cup by a sensitive electrometer. The uncertainty in the detector calibration was estimated to be less than 3%. A retractable Faraday cup was located 33 cm away from the target cell, allowing the measurement of the incoming Ar<sup>+</sup> ion-beam current ( $I_0$  is the number of Ar<sup>+</sup> ions incident per second on the target, typically  $\sim 5.0 \times 10^{10}$  particles/s).

Under the thin target conditions used in this experiment, the differential cross sections for the Ar<sup>2+</sup> formation were evaluated from the measured quantities by the expression

$$\frac{d\sigma(\theta)}{d\Omega} = \frac{I_f(\theta)}{I_0 n l}. \quad (1)$$

where  $n$  is the number of target atoms per unit volume (typically  $1.2 \times 10^{13}$  atoms/cm<sup>3</sup>) and  $l$  is the length of the scattering chamber ( $l = 2.5$  cm). The estimated rms error is 15%, while the total cross sections were reproducible to within 10% from day to day.

The total cross section  $\sigma$  for the production of the Ar<sup>2+</sup> particles was obtained by the numerical integration of  $d\sigma/d\Omega$  over all angles measured; this is

$$\sigma = 2\pi \int_0^{\theta_m} \frac{d\sigma}{d\Omega} \sin(\theta) d\theta. \quad (2)$$

For  $\theta > \theta_m$  the differential cross sections drop below the detection limit ( $1 \times 10^{-5}$  Å<sup>2</sup> sr<sup>-1</sup>). If we considered this detection limit as a constant contribution for angles  $\theta > \theta_m$ , we obtained an upper limit for the estimation of this contribution for all the energies of  $0.12 \times 10^{-20}$  cm<sup>2</sup>, which is less than 10% for energies above 2 keV. The apparatus angular resolution function was not deconvolute from the cross section data.

In order to estimate the nonlinear contribution of the growth curve, we calculated the cross section taking into account multiple collision. Considering a three-component system, we have (McDaniel *et al* 1993):

$$F_2 = \sigma_{12} n l + [(\sigma_{02} - \sigma_{12})\sigma_{10} - (\sigma_{12} + \sigma_{21} + \sigma_{20})\sigma_{12}](n l)^2 / 2 \quad (3)$$

where  $F_2$  is the fraction of the beam in the charge state 2. As the two electrons transfer cross sections are much less than the one electron transfer cross sections:

$$F_2 = [1 - (\sigma_{10} + \sigma_{12} + \sigma_{21})(n l / 2)](n l \sigma_{12}). \quad (4)$$

Taking  $\sigma_{10}$  (3 keV) =  $22.5$  Å<sup>2</sup> (Hegerberg *et al* 1978),  $\sigma_{21}$  (3.6 keV) =  $4.81$  Å<sup>2</sup> (Astner *et al* 1984) for the Ar<sup>+</sup> + Ar system, together with the fractions measured in this experiment at three values of  $n l$ , that being:  $F_2 = 1.21 \times 10^{-6}$  at  $n l = 1.5 \times 10^{13}$  atoms/cm<sup>2</sup>;  $F_2 = 2.55 \times 10^{-6}$  at  $n l = 3.0 \times 10^{13}$  atoms/cm<sup>2</sup> and  $F_2 = 3.87 \times 10^{-6}$  at  $n l = 4.5 \times 10^{13}$  atoms/cm<sup>2</sup>. We calculated the value of  $\sigma_{12}$  using equation (4), we obtained  $\sigma_{12} = 8.235 \times 10^{-20}$  cm<sup>2</sup>,  $8.863 \times 10^{-20}$  and  $9.22 \times 10^{-20}$  cm<sup>2</sup>, respectively, which have a maximum error of 8.5% with respect to the

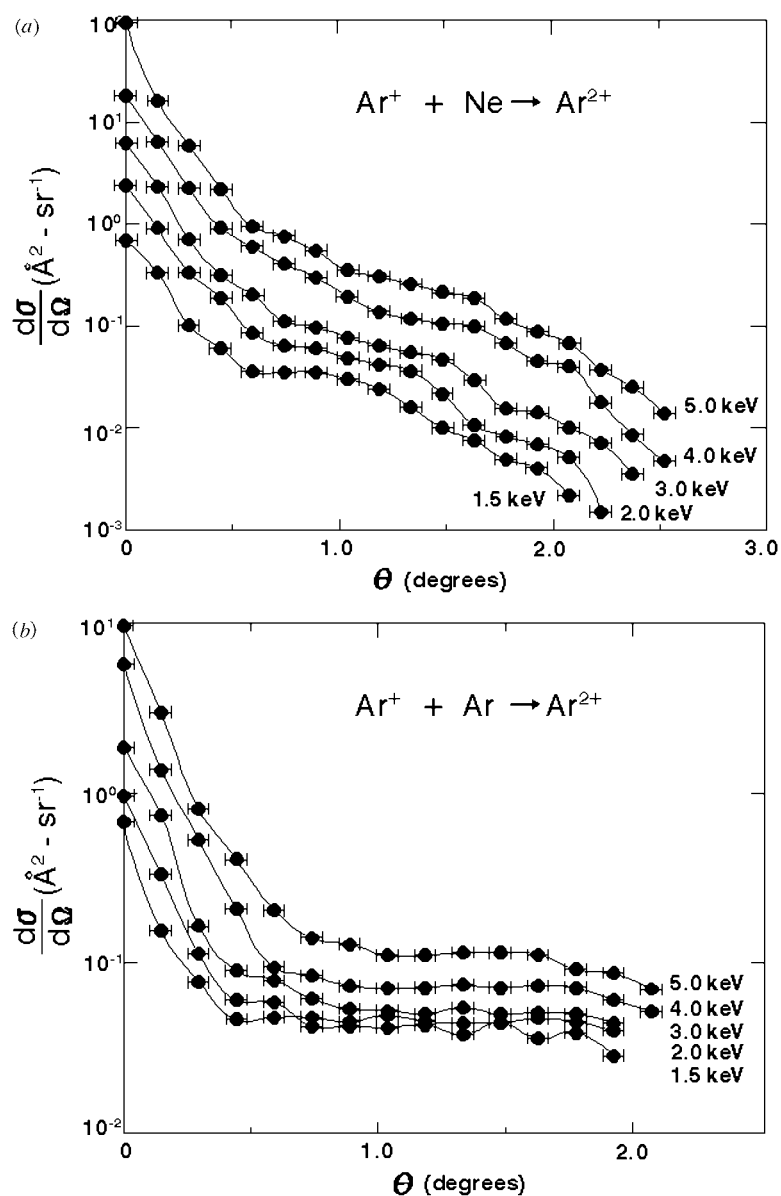


**Figure 2.** Measured absolute differential cross sections for single-electron loss of  $\text{Ar}^+$  ions in: (a) Ne; (b) Ar; (c) Kr; (d) Xe.

value obtained by integrating the angular distribution at 3.0 keV. And then the error caused by the data acquisition method and analysis is less than 10%.

Extreme care was taken when the absolute differential cross section was measured. The reported value of the angular distribution was obtained by measuring it with and without gas in the target cell with the same steady beam in order to eliminate the counting rate due to ionization of the  $\text{Ar}^+$  beam on the slits and those arising from background distributions.

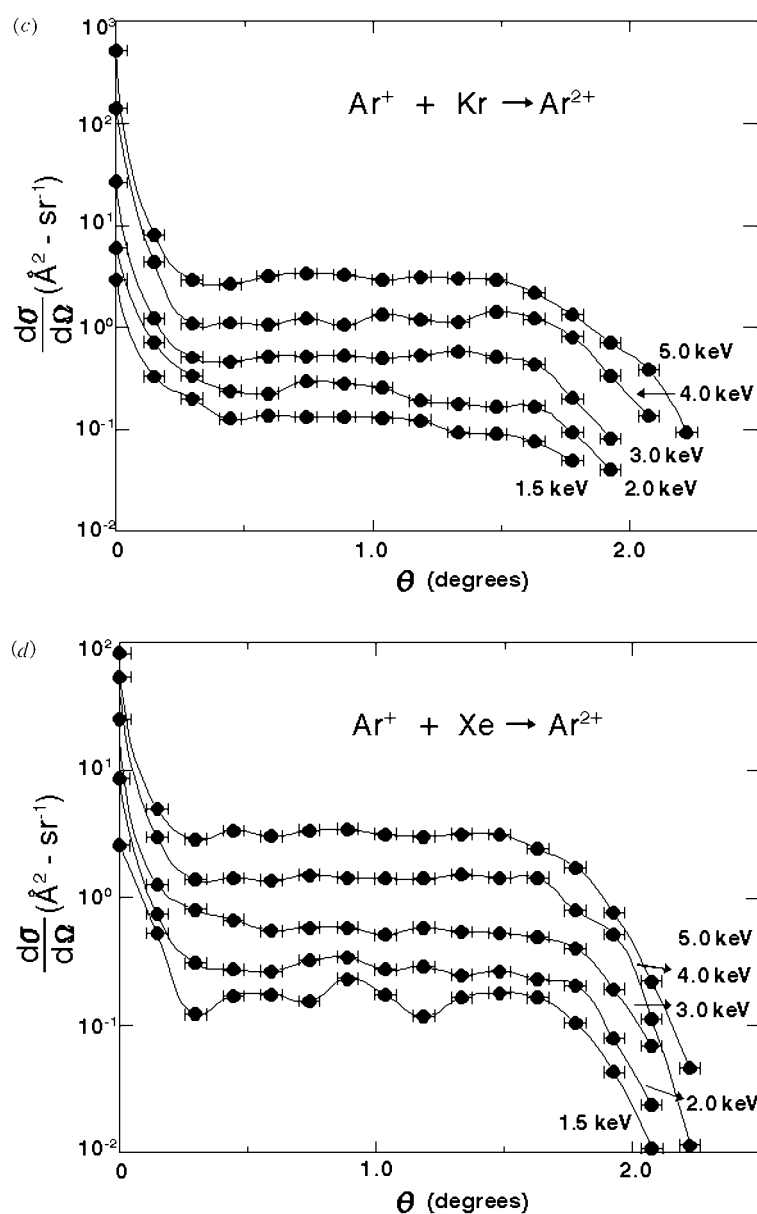
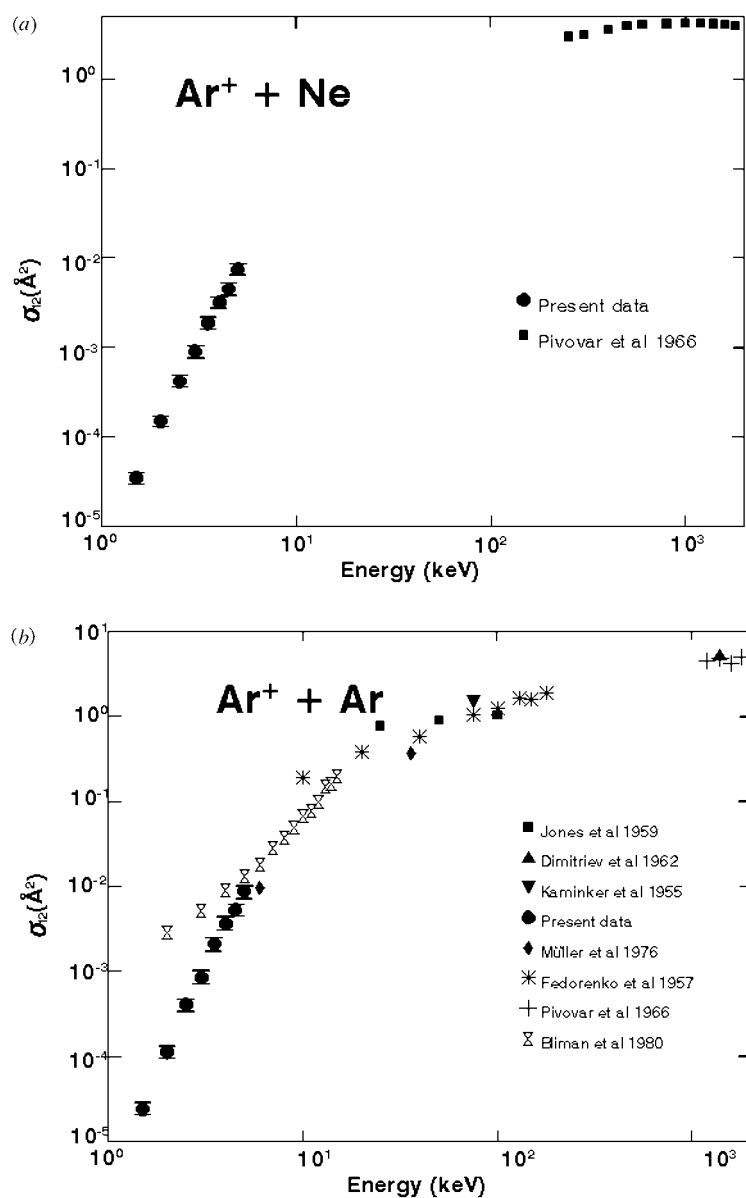


Figure 2. Continued.

In this paper, changes were not observed in the absolute values with respect to the ion source conditions. Also, no variation in the distributions was detected over a target pressure range of 0.2–0.6 mTorr.

Several sources of systematic errors are present and have been discussed in a previous paper (Martínez 1998). The absolute error of the reported cross sections is believed to be less than  $\pm 15\%$ . This estimate represents both random and systematic errors.



**Figure 3.** Total cross sections for single-electron loss of  $\text{Ar}^+$  ions in atoms: (a) Ne; (b) Ar; (c) Kr; (d) Xe.

### 3. Results and discussion

Measurements of absolute differential cross sections (DCSs) have been performed at laboratory angles of  $-3^\circ \leq \theta \leq 3^\circ$  and collision energies of  $1.5 \leq E_{\text{lab}} \leq 5.0$  keV. We show in figures 2(a)–(d), our differential cross sections for single-electron loss of  $\text{Ar}^+$  in Ne, Ar, Kr and Xe at 1.5, 2.0, 3.0, 4.0 and 5.0 keV laboratory energies. All of these curves show a monotonic decrease in the differential cross section with increasing angle. Some of the

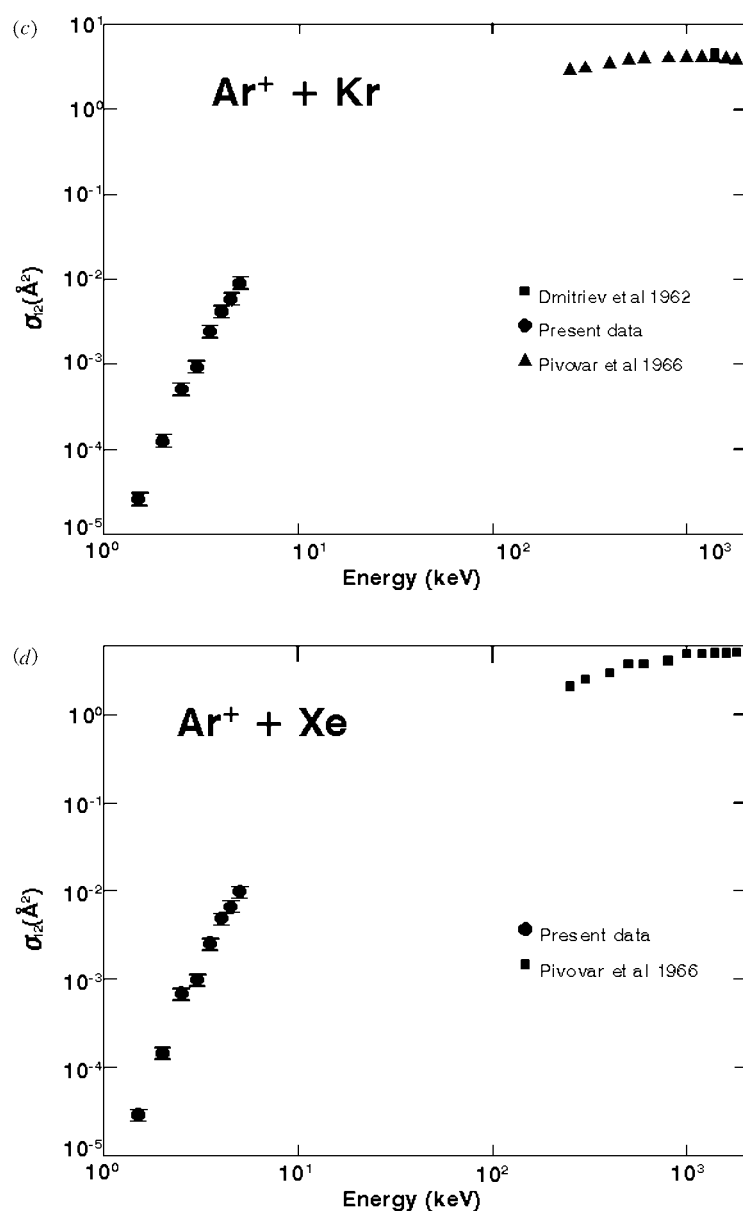
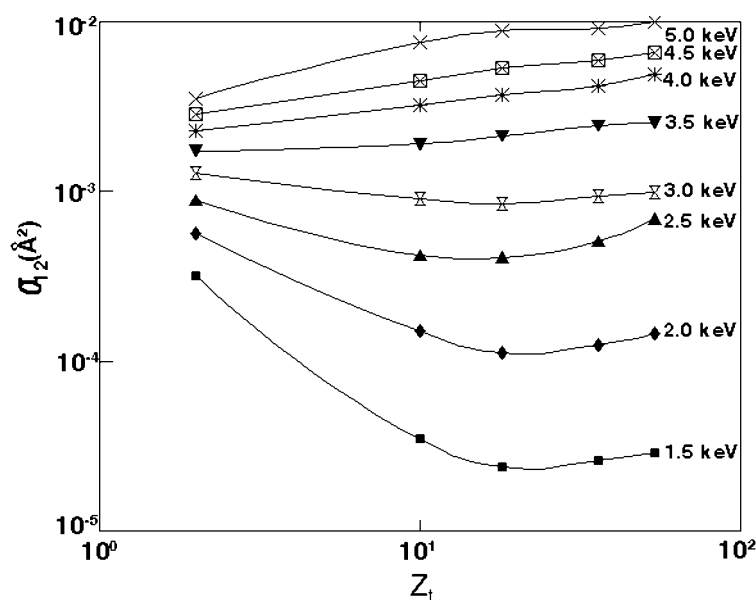


Figure 3. Continued.

electron loss data show slight structures, which tend to diminish as the incident energy increases.

A remarkable feature can be observed in figures 2(b)–(d), in all of which the total cross section displays a plateau behaviour in the angular scattering range of  $0.5$ – $1.5^\circ$ . The differential cross sections have been integrated to yield total cross sections. Table 1 gives the values of the total cross sections for the four collision systems and in figures 3(a)–(d) a comparison of our values with those of other investigators is shown. The error bars are given as an indication of the maximum reproducibility of the data in the present energy range (15%).



**Figure 4.** Total cross sections for single-electron loss of  $\text{Ar}^+$  ions in atoms as a function of the target atomic number  $Z_t$ .

The energy dependence of the single-electron loss cross section for an  $\text{Ar}^+$  ion colliding with Ne is shown in figure 3(a), together with the higher energy data of Pivovar *et al* (1966). The cross sections obtained exhibit a monotonically increasing behaviour as a function of the incident energy.

It can be seen from figure 3(b), that the shape of the cross section for an  $\text{Ar}^+$  ion colliding with Ar shows a monotonic increasing behaviour as a function of the incident energy. At energies greater than 6 keV, our data were found to merge smoothly into the cross sections measured by Müller (1976), Fedorenko *et al* (1957), Jones *et al* (1959), Kaminker and Fedorenko (1955), Bliman *et al* (1980), Pivovar *et al* (1966) and Dmitriev *et al* (1962), while at energies lower than 6 keV, the data of Bliman *et al* (1980) are 26 to 1.5 times bigger than the present data. These results give a general shape of the whole curve of single-electron loss cross sections for the  $\text{Ar}^+$ –Ar system over a wide range of energies (1.5–1800 keV).

For  $\text{Ar}^+$ –Kr systems, our total cross sections are found to be of the order of magnitude between  $10^{-5}$  and  $10^{-2} \text{ Å}^2$  (see figure 3(c)). Also the shape of the total cross sections shows a monotonic increasing behaviour as a function of the incident energy. The only previous measurements of this system were made by Dmitriev *et al* (1962) at 1400 keV and Pivovar *et al* (1966) from 1200 to 1800 keV.

For  $\text{Ar}^+$ –Xe systems, there are no previous measurements to compare with the present results. Our total cross sections are found to be of the order of magnitude between  $10^{-5}$  and  $10^{-2} \text{ Å}^2$  and show a monotonic increasing behaviour as a function of the incident energy (see figure 3(d)).

Figure 4 shows the dependence with  $Z_t$  of the electron loss cross section for 1.5–5.0 keV  $\text{Ar}^+$  ions colliding with rare-gas atoms. At high energies the electron loss shows an increasing behaviour, while at low energies it displays a decreasing behaviour as  $Z_t$  goes from 2 to 18. In all cases the present results display an experimental evidence of a smooth  $Z_t$  dependence for higher  $Z_t$  values. That is, there is a clear tendency towards a saturation for the cross sections



**Table 1.** Total electron loss cross sections  $\sigma_{12}$  ( $10^{-20}$  cm<sup>2</sup>) as a function of  $Z_t$  and the incident energy.

Target energy (keV)	Ne	Ar	Kr	Xe
1.0				
1.5	0.35	0.24	0.26	0.29
2.0	1.50	1.13	1.25	1.45
2.0		29 <sup>f</sup>		
2.5	4.20	4.09	5.10	6.90
3.0	9.00	8.50	9.30	9.90
3.0		52 <sup>f</sup>		
3.5	19.00	21.10	24.30	25.30
4.0	32.00	36.66	42.00	49.00
4.0		90 <sup>f</sup>		
4.5	45.00	52.74	59.00	66.00
5.0	75.00	87.65	90.30	99.10
5.0		130 <sup>f</sup>		
6.0		96 <sup>a</sup>		
6.0		180 <sup>f</sup>		
7.0		280 <sup>f</sup>		
8.0		380 <sup>f</sup>		
9.0		490 <sup>f</sup>		
10		1 923 <sup>b</sup>		
10		680 <sup>f</sup>		
11		780 <sup>f</sup>		
12		990 <sup>f</sup>		
13		1500 <sup>f</sup>		
14		1600 <sup>f</sup>		
15		2000 <sup>f</sup>		
20		3 846 <sup>b</sup>		
25		7 800 <sup>c</sup>		
36		3 700 <sup>a</sup>		
40		5 769 <sup>b</sup>		
50		9 200 <sup>c</sup>		
75		15 000 <sup>d</sup>		
75		10 577 <sup>b</sup>		
100		10 500 <sup>c</sup>		
100		12 500 <sup>b</sup>		
130		16 346 <sup>b</sup>		
150		15 962 <sup>b</sup>		
180		19 231 <sup>b</sup>		
250	30 000 <sup>g</sup>		30 000 <sup>g</sup>	21 000 <sup>g</sup>
300	32 000 <sup>g</sup>		32 000 <sup>g</sup>	25 000 <sup>g</sup>
400	36 000 <sup>g</sup>		36 000 <sup>g</sup>	30 000 <sup>g</sup>
500	40 000 <sup>g</sup>		40 000 <sup>g</sup>	38 000 <sup>g</sup>
600	41 000 <sup>g</sup>		41 000 <sup>g</sup>	38 000 <sup>g</sup>
800	42 000 <sup>g</sup>		42 000 <sup>g</sup>	41 000 <sup>g</sup>
1000	43 000 <sup>g</sup>		43 000 <sup>g</sup>	49 000 <sup>g</sup>
1200	43 000 <sup>g</sup>	45 000 <sup>g</sup>	43 000 <sup>g</sup>	49 000 <sup>g</sup>
1400	42 000 <sup>g</sup>	48 000 <sup>g</sup>	42 000 <sup>g</sup>	50 000 <sup>g</sup>
1400		54 000 <sup>c</sup>	46 000 <sup>c</sup>	

**Table 1.** Continued.

Target energy (keV)	Ne	Ar	Kr	Xe
1600	41 000 <sup>g</sup>	42 000 <sup>g</sup>	41 000 <sup>g</sup>	50 000 <sup>g</sup>
1800	40 000 <sup>g</sup>	50 000 <sup>g</sup>	40 000 <sup>g</sup>	51 000 <sup>g</sup>

<sup>a</sup> Müller *et al* (1976).<sup>b</sup> Fedorenko *et al* (1957).<sup>c</sup> Jones *et al* (1959).<sup>d</sup> Kaminker and Fedorenko (1955).<sup>e</sup> Dmitriev *et al* (1962).<sup>f</sup> Bliman *et al* (1980).<sup>g</sup> Pivovarov *et al* (1966).

as  $Z_t$  increases. A saturation of the loss cross section for high  $Z_t$  has been observed for  $\text{He}^+$  (Melo *et al* 1999, Voitkiv *et al* 1999, Santa'Anna *et al* 1995, Kaneko 1985), for  $\text{C}^{3+}$  and  $\text{O}^{5+}$  (Melo *et al* 1999) and for  $\text{Kr}^+$  (Martínez *et al* 2000) as projectiles and in the excitation channel of highly charged projectiles (Kaneko 1985, Wohrer *et al* 1986) on neutral targets.

It thus appears desirable that a detailed theoretical analysis be carried out to further check this behaviour.

#### 4. Summary

The results of this paper can be summarized as follows:

- (a) Differential and total cross sections for electron loss in  $\text{Ar}^+$ –atom collisions were obtained at laboratory energies between 1.5 and 5.0 keV.
- (b) The electron loss cross sections for all the targets studied are found to be of the order of magnitude between  $10^{-22}$  and  $10^{-20}$   $\text{cm}^2$ , and show a monotonically increasing behaviour as a function of the incident energy.
- (c) A striking feature of the results is the experimental evidence of a saturation in the electron loss cross section as the nuclear charge of the target increases.

#### Acknowledgments

We are grateful to B E Fuentes and A Amaya-Tapia for helpful suggestions and comments, and thank José Rangel and A González for their technical assistance. Research supported by DGAPA IN-100392 and CONACYT 32175-E.

#### References

- Astner G, Bárány A, Cederquist H, Danared H, Hultdt S, Hvelplund P, Johnson A, Knudsen H, Liljeby L and Rensfelt K-G 1984 *J. Phys. B: At. Mol. Phys.* **17** L877–83
- Barat M and Lichten W 1972 *Phys. Rev. A* **6** 211–29
- Brenot J C, Dhuicq D, Gauyacq J P, Pommier J, Sidis V, Barat M and Pollack E 1975 *Phys. Rev. A* **11** 1245–66
- Bliman S, Chan-Tung N, Dousson S, Jacquot B and Van Houtte D 1980 *Phys. Rev. A* **21** 1856–62
- Datz S, Drake G W F, Gallagher T F, Kleinpoppen H and Putitz Zu G 1999 *Rev. Mod. Phys.* **71** S223–41
- Delos J 1981 *Rev. Mod. Phys.* **53** 287–357
- Dmitriev I S, Nikolaev V S, Fateeva L N and Teplova Ya 1962 *Sov. Phys.-JETP* **15** 11–7
- Fedorenko N V, Afrosimov V V and Kaminker D A 1957 *Sov. Phys.-Tech. Phys.* **1** 1861–71
- Hegerberg R, Thórarinn S and Elford M T 1978 *J. Phys. B: At. Mol. Phys.* **11** 133–47
- Jalowiy T, Jakubaša-Amundsen D H, Lucas M W and Groeneveld K O 2000 *Phys. Rev. A* **61** 022714-1-9

- Janev R K 1995 *Atomic and Molecular Processes in Fusion Edge Plasma* (New York: Plenum)
- Jones P R, Ziemba F P, Moses H A and Everhart E 1959 *Phys. Rev.* **113** 182–91
- Kaminker D M and Fedorenko N V 1955 *Zh. Tekh. Fiz.* **25** 2239
- Kaneko T 1985 *Phys. Rev. A* **32** 2175–85
- 1986 *Phys. Rev. A* **34** 1779–86
- Kolakowska A and Pindzola M S 1999 *Phys. Rev. A* **59** 3588–91
- Lichten W 1967 *Phys. Rev.* **164** 131–42
- Martínez H 1999 *J. Phys. B: At. Mol. Opt. Phys.* **32** 189–96
- 1998 *J. Phys. B: At. Mol. Opt. Phys.* **31** 1553–62
- Martínez H, Amaya-Tapia A and Hernández J M 2000 *J. Phys. B: At. Mol. Opt. Phys.* **33** 1935–42
- Martínez H and Reyes P G 1999 *Phys. Rev. A* **59** 2504–7
- McDaniel E W, Mitchell J B A and Rudd M E 1993 *Atomic Collisions* (New York: Wiley)
- Melo W S, Sant’Anna M M, Santos A C F, Sigaud G M and Montenegro E C 1999 *Phys. Rev. A* **60** 1124–34
- Möller W 1999 *Final Programme and Abstract of the 14th Int. Conf. on Ion Beam Analysis and 6th Eur. Conf. on Accelerators in Applied Research and Technology*
- Montenegro C, Meyerhof W E and McGuire J H 1994 *Adv. At. Mol. Opt. Phys.* **34** 249
- Müller A, Klinger H and Salzborn E 1976 *J. Phys. B: At. Mol. Phys.* **9** 291–3
- Pivovarov L I, Novikov M T and Dolgov A S 1966 *Sov. Phys.-JETP* **23** 357–62
- Ogawa H, Sakamoto N and Tsuchida H 2000 *Nucl. Instrum. Methods B* **164–5** 279–83
- Saha A K, Tribedi L C, Ram K V T, Prasad K G and Tandon P N 1999 *Phys. Scr. T* **80B** 384–6
- Sant’Anna M M, Melo W S, Santos A C F, Sigaud G M and Montenegro E C 1995 *Nucl. Instrum. Methods B* **99** 46–9
- Sant’Anna M M, Melo W S, Santos A C F, Sigaud G M, Montenegro E C, Shah M B and Meyerhof W E 1998 *Phys. Rev. A* **58** 1204–11
- Sidis V, Barat M and Dhuicq D 1975 *J. Phys. B: At. Mol. Phys.* **8** 474–93
- Voitkiv A B, Sigaud G M and Montenegro E C 1999 *Phys. Rev. A* **59** 2794–803
- Wohrer K, Chetoui A, Rozet J P, Jolly A, Fernandez F, Stephan C, Brendlé B and Gayet R 1986 *J. Phys. B: At. Mol. Phys.* **19** 1997–2006
- Wu W *et al* 1997 *Phys. Rev. A* **55** 2771–7